RSC Advances

Heteroleptic copper(I) sensitizers with one versus two hole-transporting units in functionalized 2,9-dimethyl-1,10-phenanthroline ancillary ligands

Journal:	*RSC Advances*
Manuscript ID:	RA-ART-06-2015-012296.R1
Article Type:	Paper
Date Submitted by the Author:	05-Aug-2015
Complete List of Authors:	Housecroft, Catherine; University of Basel, Department of Chemistry Constable, Edwin; University of Basel, Departement Chemie Fuerer, Sebatian; University of Basel, Departement Chemie Bozic-Weber, Biljana; University of Basel, Department of Chemistry Neuburger, Markus; University of Basel, Department of Chemistry

RSC Advances

RSCPublishing

ARTICLE

Heteroleptic copper(I) sensitizers with one versus two hole-transporting units in functionalized 2,9-dimethyl-1,10-phenanthroline ancillary ligands

Cite this: DOI: 10.1039/x0xx00000x

Received 00th January 2012,
Accepted 00th January 2012

DOI: 10.1039/x0xx00000x

www.rsc.org/

Sebastian O. Fürer,[a] Biljana Bozic-Weber,[a] Markus Neuburger,[a] Edwin C. Constable[a] and Catherine E. Housecroft*[a]

A series of homoleptic $[Cu(L)_2][PF_6]$ complexes in which L is a 2,9-dimethyl-1,10-phenanthroline fused at the 5,6-positions with a 2'-functionalized imidazole (ligands **1–4**), or substituted in the 4,7-positions with electron-donating 4-(diphenylamino)phenyl groups (ligand **5**) is described; the imidazole 2'-functionality in **1** is 4-bromophenyl, in **2** is 4-(diphenylamino)phenyl, in **3** is 4-(bis(4-*n*-butoxy)phenylamino)phenyl, and in **4** is 4-(carbazol-9-yl)phenyl. The copper complexes were characterized by mass spectrometry, NMR and absorption spectroscopies and cyclic voltammetry; the single crystal structure of ligand **4** has been determined. Compared to the solution absorption spectra of $[Cu(\mathbf{1})_2][PF_6]$, $[Cu(\mathbf{2})_2][PF_6]$, $[Cu(\mathbf{3})_2][PF_6]$ and $[Cu(\mathbf{4})_2][PF_6]$, that of $[Cu(\mathbf{5})_2][PF_6]$ shows increased absorbance at wavelengths >375 nm. An on-surface strategy was used to assemble heteroleptic $[Cu(\mathbf{6})(L)]^+$ dyes on TiO_2 electrodes where **6** is ((6,6'-dimethyl-[2,2'-bipyridine]-4,4'-diyl)bis(4,1-phenylene))bis(phosphonic acid); solid-state absorption spectra confirmed enhanced light-harvesting between 375–600 nm for $[Cu(\mathbf{6})(\mathbf{5})]^+$ with respect to $[Cu(\mathbf{6})(\mathbf{1})]^+$, $[Cu(\mathbf{6})(\mathbf{2})]^+$, $[Cu(\mathbf{6})(\mathbf{3})]^+$ and $[Cu(\mathbf{6})(\mathbf{4})]^+$. Comparison of the performances of dye-sensitized solar cells (DSCs) containing $[Cu(\mathbf{6})(\mathbf{2})]^+$, $[Cu(\mathbf{6})(\mathbf{3})]^+$ and $[Cu(\mathbf{6})(\mathbf{4})]^+$ with those with $[Cu(\mathbf{6})(\mathbf{1})]^+$ indicate only a marginal influence of the diphenylamine or carbazole hole-transporting domains in 5,6-substituted phenanthroline dyes. The introduction of the 4-(diphenylamino)phenyl hole-transporting units in the 4- and 7-positions of the phen unit in **5** proves to be beneficial, with DSCs containing $[Cu(\mathbf{6})(\mathbf{5})]^+$ performing better than those with the other four dyes; duplicate DSCs were tested for each dye to validate the results. While the values of the maximum external quantum efficiencies (EQE_{max}) for $[Cu(\mathbf{6})(\mathbf{1})]^+$ and $[Cu(\mathbf{6})(\mathbf{4})]^+$ are greater than for $[Cu(\mathbf{6})(\mathbf{5})]^+$, the extension of the EQE spectrum for $[Cu(\mathbf{6})(\mathbf{5})]^+$ to longer wavelengths results in higher short-circuit current densities (J_{SC}) compared to DSCs with $[Cu(\mathbf{6})(\mathbf{1})]^+$, $[Cu(\mathbf{6})(\mathbf{2})]^+$, $[Cu(\mathbf{6})(\mathbf{3})]^+$ and $[Cu(\mathbf{6})(\mathbf{4})]^+$.

Introduction

The development of dye-sensitized solar cells (DSCs) has progressed from the prototype ruthenium dyes of Grätzel and O'Regan,[1,2] to the use of organic[3] and porphyrin-containing[4] dyes with solar-to-electrical power conversion efficiencies (PCEs) reaching ≈12%.[5] Recently, perovskite DSCs have excited considerable attention, with PCEs of 18–20%.[6,7,8] Our contributions to the advancement of DSCs focus on sustainable components,[9] in particular with copper-containing dyes[10] replacing those containing precious metals. The potential of copper(I) dyes was first recognized by Sauvage and coworkers,[11] and in 2014, PCEs exceeding 3% (relative to ≈7.5% for reference dye N719) were achieved.[12,13] Homoleptic copper(I) complexes have also been used as redox mediators combined with ruthenium(II) sensitizers in DSCs.[14]

The simplest copper(I) sensitizers are homoleptic complexes of type $[Cu(L_{anchor})_2]^+$ in which L_{anchor} is typically a diimine ligand bearing a carboxylic or phosphonic acid substituent to anchor the dye to the semiconductor surface.[15] Dye performance is most easily improved and tuned by employing heteroleptic $[Cu(L_{anchor})(L_{ancillary})]^+$ dyes, although these are often difficult to isolate because of the lability of bis(diimine)copper(I) complexes.[16] Two approaches to access heteroleptic dyes are now successfully used. The first is the

HETPHEN strategy[17] introduced by Odobel and coworkers[13,18] which relies on bulky ligands to hinder ligand exchange. Using this approach, a remarkable efficiency of 4.66% (relative to 7.36% for N719) has been recorded for the dye shown in Scheme 1a in the presence of the co-adsorbant chenodeoxycholic acid.[13] A second route to heteroleptic dyes is our 'surface-as-ligand, surface-as-complex' approach[1920,21,22] which involves a stepwise assembly of heteroleptic metal complex dyes on electrode surfaces and has been used for both copper(I)[22] and zinc(II)[23] sensitizers. The strategy provides a straightforward means for rapid screening of different combinations of anchoring and ancillary ligands. To assemble a $[Cu(L_{anchor})(L_{ancillary})]^+$ dye, an electrode is initially soaked in a solution of L_{anchor}, and then the functionalized electrode is immersed in a dye-bath containing either $[Cu(L_{ancillary})_2]^+$ or a mixture of $[Cu(MeCN)_4]^+$ and $L_{ancillary}$.[22,24]

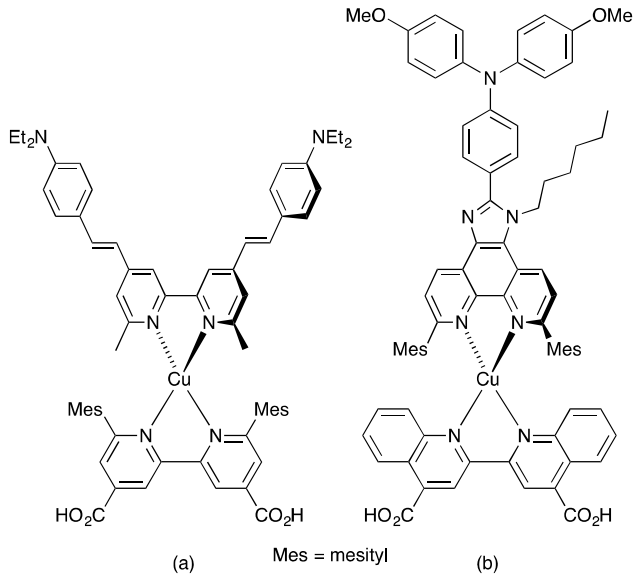

Scheme 1. Copper(I) sensitizers reported by Odobel and coworkers (see text).

The incorporation of imidazo[4',5':5,6]-1,10-phenanthroline ligands bearing electron-donating groups in the 2'-position has been shown to be advantageous in ruthenium-based sensitizers,[25] and these ligands are also attractive for copper(I)-based DSCs.[18,26] The imidazo[4',5':5,6]-1,10-phenthroline unit is readily extended with a 4-(diphenylamino)phenyl[18] or other hole-transporting unit, and Scheme 1b shows a copper(I) sensitizer which is noteworthy for its broad absorption spectrum extending beyond 700 nm; however, DSCs containing this dye gave efficiencies of <0.3% (with respect to 6.55% for N719).[18] Ligand **1**[26] (Scheme 2) is a convenient precursor to 2'-functionalized 2,9-dimethyl-imidazo[4',5':5,6]-1,10-phenthrolines for use as ancillary ligands in $[Cu(L_{anchor})(L_{ancillary})]^+$ dyes. The 2,9-substituents in the phen metal-binding domain stabilize copper(I) with respect to oxidation by sterically hindering the transformation of tetrahedral copper(I) to square planar copper(II). An additional feature of **1** is the long *N*-alkyl substituent which helps to prevent intermolecular aggregation of dye molecules on the semiconductor surface and also militates against charge recombination processes.[27]

We now report the development of heteroleptic copper(I) dyes for DSCs with ancillary ligands derived through postfunctionalization of the peripheral bromo-substituent in **1**. We also demonstrate the effects of introducing hole-transporting domains into the 4- and 7-positions of 2,9-dimethyl-1,10-phenanthroline.

Experimental

General

^{1}H and ^{13}C NMR spectra were recorded at 295 K on a Bruker Avance III-500 NMR spectrometer with chemical shifts referenced to residual solvent peaks with respect to δ(TMS) = 0 ppm. Solution and solid-state absorption spectra were recorded on Perkin Elmer Lambda 25 and Cary 5000 spectrophotometers, respectively, and FT-IR spectra on a Perkin Elmer Spectrum Two spectrometer equipped with a UATR. Electrospray (ESI) mass spectra (solution samples in MeOH with a drop of CH_2Cl_2 added) and high resolution ESI-MS were measured on Bruker Esquire 3000^{plus} and Bruker maXis 4G instruments, respectively.

Electrochemical measurements were performed on a CHI 900B instrument by cyclic voltammetry (CV) using a glassy carbon working electrode, platinum wire auxiliary electrode, and a silver wire pseudo-reference electrode. HPLC grade, argon degassed CH_2Cl_2 solutions ($\approx 10^{-4}$ mol dm^{-3}) of the copper complexes were used with 0.1 M $[^nBu_4N][PF_6]$ as supporting electrolyte; the scan rate was 0.1 V s^{-1} and ferrocene was used as an internal standard, added at the end of each experiment.

Ligands and complexes

Compound **1**,[26] **2**,[26] 2,9-dimethyl-1,10-phenanthroline-5,6-dione,[28] 4-(9*H*-carbazol-9-yl)benzaldehyde,[29] 4,7-dichloro-2,9-dimethyl-1,10-phenanthroline,[30] $[Cu(MeCN)_4][PF_6]$[31] and $[Cu(\mathbf{2})_2][PF_6]$[26] were synthesized as previously reported. 4,4'-Di-n-butoxydiphenylamine was prepared by the method reported for the analogous hexoxy derivative,[32] and NMR spectra corresponded to those published.[33] Bis(dibenzylideneacetone)palladium(0), $[Pd(dba)_2]$ was purchased from Strem Chemicals, and 4-(*N,N*-diphenylamino)phenylboronic acid from Fluorochem.

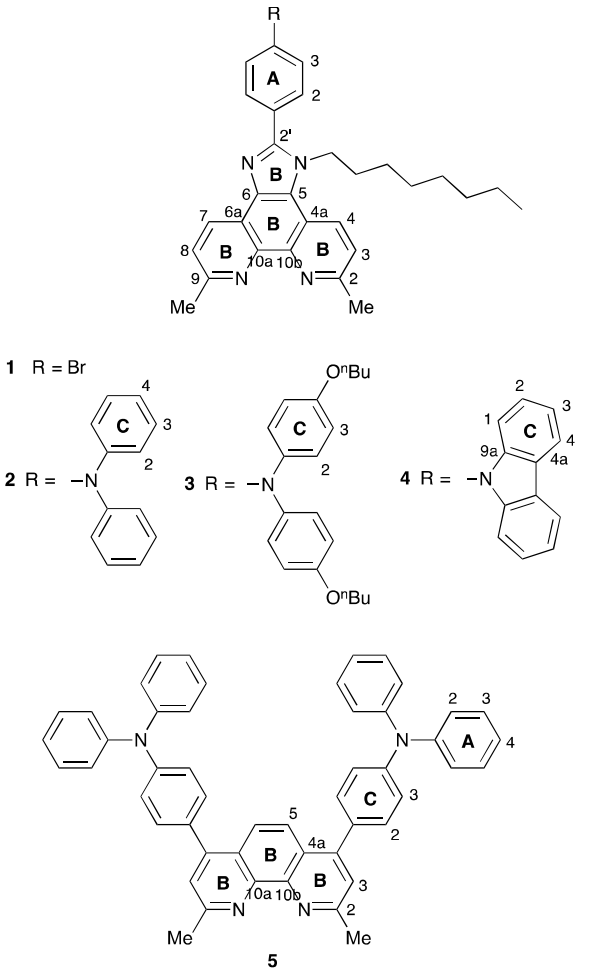

Scheme 2. Structures of ligands **1–5**. Ring labelling is for NMR assignments.

Compound 3. A flask (50 ml) was charged with **1** (300 mg, 0.582 mmol), 4,4'-di-n-butoxydiphenylamine (279 mg, 0.873 mmol), NaO^{t}Bu (140 mg, 1.45 mmol) and a catalytic amount of [Pd(dba)$_2$] (18.4 mg, 0.0291 mmol) and was evacuated for 15 min. Toluene (20 ml) and P^{t}Bu$_3$ (0.03 ml of a 0.1 M sol. in toluene, 23.9 mg, 0.0291 mmol) were added and the reddish brown mixture was heated to 95 °C for 8 days. The mixture was allowed to cool to room temperature, filtered and the solvent was removed. The remaining brown solid was purified by column chromatography on alumina eluting with CH_2Cl_2 to yield the product as a yellow solid (223 mg, 298 mmol, 51.2%). ^{1}H NMR (500 MHz, $CDCl_3$) δ / ppm 9.24 (br, 1H, H$^{B4/B7}$), 8.48 (d, J = 8.6 Hz, 1H, H$^{B4/B7}$), 7.66 (d, J = 8.2 Hz, 1H, H$^{B3/B8}$), 7.62 (d, J = 8.4 Hz, 1H, H$^{B3/B8}$), 7.54 (m, 2H, H^{A2}), 7.13 (m, 4H, H^{C2}), 7.03 (m, 2H, H^{A3}), 6.88 (m, 4H, H^{C3}), 4.64 (m, 2H, H^{NCH_2}), 3.96 (t, J = 6.5 Hz, 4H, H^{OCH_2}), 3.07 (s, 3H, H$^{Me\text{-}phen}$), 3.01 (s, 3H, H$^{Me\text{-}phen}$), 1.95 (m, 2H, H$^{NCH_2C\boldsymbol{H}_2}$), 1.78 (m, 4H, H$^{OCH_2C\boldsymbol{H}_2}$), 1.51 (m, 4H, H$^{OCH_2CH_2C\boldsymbol{H}_2}$), 1.30–1.16 (m, 10H, H$^{CH_2\text{-}octyl}$), 0.99 (t, J = 7.4 Hz, 6H, H$^{Me\text{-}butyl}$), 0.85 (t, J = 6.9 Hz, 3H, H$^{Me\text{-}octyl}$). ^{13}C NMR (126 MHz, $CDCl_3$) δ / ppm 157.5 (C^{B2+B9}), 156.1 (C^{C4}), 139.6 (C^{C1}), 130.6 (C^{A2}), 128.7 (C$^{B4/B7}$), 127.6 (C^{C2}), 124.5 (C$^{B3/B8}$), 123.6 (C$^{B3/B8}$), 118.6 (C^{A3}), 117.5 (C$^{B4a/B6a}$), 115.6 (C^{C3}), 67.9 (C^{OCH_2}), 46.9 (C^{NCH_2}), 31.8 (C$^{CH_2\text{-}octyl}$), 31.5 (C$^{OCH_2C\boldsymbol{H}_2}$), 30.2, (C$^{NCH_2C\boldsymbol{H}_2}$), 29.2 (C$^{CH_2\text{-}octyl}$), 29.0 (C$^{CH_2\text{-}octyl}$), 26.4 (C$^{CH_2\text{-}octyl}$), 25.3 (C$^{phen\text{-}Me}$), 25.1 (C$^{phen\text{-}Me}$), 22.7 (C$^{CH_2\text{-}octyl}$), 19.4 (C$^{OCH_2CH_2C\boldsymbol{H}_2}$), 14.2 (C$^{Me\text{-}octyl}$), 14.0 (C$^{Me\text{-}butyl}$), (other C^Q not resolved). UV-Vis (CH_2Cl_2, 1.00 × 10^{-5} mol dm^{-3}) λ / nm (ε / dm^3 mol^{-1} cm^{-1}) 267 (35700), 296 (40700), 341 sh (23800). HR ESI-MS *m/z*: 748.4582 [M+H]$^+$ (calc. 748.4585). Found C 78.52, H 7.51, N 8.96; $C_{49}H_{57}N_5O_2$ requires C 78.68, H 7.68, N 9.36%.

Compound 4a. 4-(9*H*-Carbazol-9-yl)benzaldehyde (535 mg, 1.97 mmol), 2,9-dimethyl-1,10-phenanthroline-5,6-dione (481 mg, 2.02 mmol) and an excess of NH_4OAc (5.04 g, 65.4 mmol) were added to EtOH (100 ml). The yellow mixture was heated at reflux overnight after which time the solvent was removed. The remaining orange solid was washed with water and Et_2O. The product was purified using column chromatography (alumina, CH_2Cl_2 with 3% MeOH) and was isolated as a yellow solid (282 mg, 0.575 mmol, 29.2%). ^{1}H NMR (500 MHz, DMSO-d_6) δ / ppm 13.8 (br, NH), 8.84 (d, J = 8.2 Hz, 2H, H^{B4}), 8.56 (m, 2H, H^{A2}), 8.29 (m, 2H, H^{C4}), 7.91 (m, 2H, H^{A3}), 7.72 (m, 2H, H^{B3}), 7.55 (m, 2H, H^{C1}), 7.49 (m, 2H, H^{C2}), 7.34 (m, 2H, H^{C3}), 2.82 (s, 6H). ^{13}C NMR (126 MHz, DMSO-d_6) 156.0 (C^{B2}), 149.3 (C$^{imid\text{-}2}$), 143.1 (C^{B10a}), 139.8 (C^{C9a}), 137.6 (C^{A4}), 129.9 (C^{B4}), 129.0 (C^{A1}), 127.6 (C^{A2}), 126.9 (C^{A3}), 126.5 (C^{B5}), 126.3 (C^{C2}), 123.2 (C^{B3}), 120.5 (C^{C4}), 120.2 (C^{C3}), 109.6 (C^{C1}), 24.7 (C^{Me}), (C^{B4a} not resolved). ESI MS *m/z*: 490.4 [M+H]$^+$ (calc. 490.2)

Compound 4. NaH (60% oil dispersion, 122 mg, 3.05 mmol) was suspended and stirred vigorously for 1.5 h in DMF (5 ml) under N_2. Compound **4a** (200 mg, 0.409 mmol) was added and the suspension was stirred for 10 min. Then 1-bromo-*n*-octane (0.711 ml, 789 mg, 4.09 mmol) was added and the mixture was heated at 70 °C for 3 days. The black mixture was allowed to cool to room temperature and was diluted with water, giving a suspension which was extracted with CH_2Cl_2 (25 ml). The organic layer was washed with water (5 × 40 ml), dried over Na_2SO_4 and the solvent was removed. The remaining DMF was removed by azeotrope distillation with toluene five times. The brown residue was washed with petroleum ether and dried *in vacuo*. This gave a brown foam which was purified by column chromatography (three columns: alumina, CH_2Cl_2 changing to CH_2Cl_2/2% MeOH; alumina, toluene/ethyl acetate 4:1 changing to 1:1; alumina, CH_2Cl_2/0.25% MeOH). Compound **4** was isolated as a beige solid (45 mg, 0.075 mmol, 18.3%). ^{1}H NMR (500 MHz, DMSO-d_6) δ / ppm: 8.85 (d, J = 8.3 Hz, 1H, H^{B7}), 8.78 (d, J = 8.6 Hz, 1H, H^{B4}), 8.30 (d, J = 7.9 Hz, 2H, H^{C4}), 8.10 (m, 2H, H^{A2}), 7.91 (m, 2H, H^{A3}), 7.77 (d, J = 8.3 Hz, 1H, H^{B3}), 7.73 (d, J = 8.0 Hz, 1H, H^{B8}), 7.56 (d, J = 8.2 Hz, 2H, H^{C1}), 7.50 (t, J = 7.6 Hz, 2H, H^{C2}), 7.35 (t, J = 7.3 Hz, 2H H^{C3}), 4.82 (m, 2H, H^{NCH_2}), 2.84 (s, 3H, H$^{Me\text{-}phen}$), 2.83 (s, 3H, H$^{Me\text{-}phen}$), 1.85 (m, 2H, H$^{NCH_2C\boldsymbol{H}_2}$), 1.15–1.05 (m, 10H, H^{CH_2}), 0.68 (m, 3H, H$^{Me\text{-}octyl}$). ^{13}C NMR (126 MHz, DMSO-d_6) δ / ppm: 156.2 (C$^{B2/B9}$), 155.7 (C$^{B2/B9}$), 152.4 (C$^{imid\text{-}2}$), 139.7 (C^{C9a}), 137.8 (C^{A4}), 131.6 (C^{A2}), 130.0 (C^{B7}), 129.3 (C^{B4}), 129.2 (C^{A1}), 126.6 (C^{A3}), 126.2 (C^{C2}), 124.4 (C^{B5}), 123.5 (C^{B8}), 123.0 (C^{B3}), 122.8 (C^{C4a}), 121.4 (C^{B6a}), 120.5 (C^{C4}), 120.3 (C^{C3}), 117.4 (C^{B4a}), 109.5 (C^{C1}), 45.7 (C^{NCH_2}), 30.9 (C^{CH_2}), 28.9 (C$^{NCH_2C\boldsymbol{H}_2}$),

28.0 (C^{CH_2}), 25.0 (C^{CH_2}), 24.6 (overlapping $C^{Me\text{-}phen}$), 21.7 (C^{CH_2}), 18.4 (C^{CH_2}), 13.6 ($C^{Me\text{-}octyl}$), (C^{B6}, C^{B10a}, C^{B10b} not resolved). UV-Vis (CH_2Cl_2, 1.00×10^{-5} mol dm^{-3}) λ / nm (ε / dm^3 mol^{-1} cm^{-1}) 294 (55000), 310 sh (35500), 325 sh (29900), 340 (23000), 370 sh (4200). ESI MS *m/z*: 602.6 $[M+H]^+$ (calc. 602.3). Found: C 78.95, H 6.56, N 10.80; $C_{41}H_{39}N_5 \cdot H_2O$ requires C 79.45, H 6.67, N 11.30%.

Compound 5. K_3PO_4 (343 mg, 1.62 mmol) was dissolved in H_2O (2 ml) under N_2, and N_2 was bubbled through the solution for 10 min. In a separate flask, N_2 was bubbled through 1,4-dioxane (5 ml) for 10 min and then 4,7-dichloro-2,9-dimethyl-1,10-phenanthroline (100 mg, 0.361 mmol), 4-(diphenylamino)phenylboronic acid (230 mg, 0.794 mmol) and catalytic amounts of $[Pd(dba)_3]$ (24.7 mg, 0.0238 mmol, 6.6 mol%) and tricyclohexylphosphine (15.2 mg, 0.0542 mmol) were added. The aqueous solution of K_3PO_4 was then added to the reaction mixture and this was heated at reflux at 95 °C for 15 h. The orange mixture was allowed to cool down to room temperature and water (10 ml) was added. The mixture was extracted with CH_2Cl_2 (5 × 15 ml) and the organic layer was dried over Na_2SO_4 and the solvent then removed. The product was recrystallized from CH_2Cl_2/MeOH (1 : 1) and **5** was isolated as a yellow solid (97.0 mg, 0.140 mmol, 38.7%). ^{1}H NMR (500 MHz, $CDCl_3$) δ / ppm 8.00 (s, 2H, H^{B5}), 7.55 (s, 2H, H^{B3}), 7.41 (m, 4H, H^{C2}), 7.32 (m, 8H, H^{A3}), 7.19 (m, 12H, H^{A2+C3}), 7.10 (m, 4H, H^{A4}), 3.14 (s, 6H, H^{Me}).^{13}C (126 MHz, $CDCl_3$) δ / ppm 158.8 (C^{B2}), 150.2 (C^{B4}), 148.9 (C^{C4}), 147.3 (C^{A1}), 142.9 (C^{B10a}), 130.8 (C^{C2}), 129.7 (C^{A3}), 125.2 (C^{A2}), 125.1 (C^{B4a}), 124.8 (C^{B3}), 123.9 (C^{A4}), 123.5 (C^{B5}), 122.5 (C^{C3}), 24.7 (C^{Me}), (C^{C1} not resolved). UV-Vis (CH_2Cl_2, 1.00×10^{-5} mol dm^{-3}) λ / nm (ε / dm^3 mol^{-1} cm^{-1}) 297 (49000), 360 sh (18100), 500 sh (4950). HR ESI-MS *m/z*: 695.3174 $[M+H]^+$ (calc. 695.3169) Satisfactory elemental analysis was not obtained.

[Cu(1)$_2$][PF$_6$]. A solution of $[Cu(NCMe)_4][PF_6]$ (16.2 mg, 0.0435 mmol) in MeCN (2 mL) was added dropwise to a solution of **1** (44.8 mg, 0.0870 mmol) in $CHCl_3$ (1 mL). The dark red solution was stirred for 3h and then the solvent was removed. The product was purified by column chromatography (alumina, CH_2Cl_2 with 1% MeOH) and $[Cu(\mathbf{1})_2][PF_6]$ was isolated as a dark red solid (38.0 mg, 0.0310 mmol, 70.5%). ^{1}H NMR (500 MHz, CD_3CN) δ / ppm 9.10 (d, J = 8.2 Hz, 2H, H^{B7}), 8.91 (d, J = 8.7 Hz, 2H, H^{B4}), 7.91 (d, J = 8.6 Hz, 2H, H^{B3}), 7.89 (d, J = 8.3 Hz, 2H, H^{B8}), 7.82 (m, 4H, H^{A3}), 7.73 (m 4H, H^{A2}), 4.73 (t, J = 7.3 Hz, 4H, H^{NCH_2}), 2.44 (s, 6H, $H^{Me\text{-}phen}$), 2.43 (s, 6H, $H^{Me\text{-}phen}$), 1.91 (m, 4H, H^{CH_2}), 1.24–1.18 (m, 8H, H^{CH_2}), 1.16–1.11 (m, 12H, H^{CH_2}), 0.83 (t, J = 7.2 Hz, 6H, $H^{Me\text{-}octyl}$). ^{13}C NMR (126 MHz, CD_3CN) δ / ppm 157.1 ($C^{B2/B9}$), 156.6 ($C^{B2/B9}$), 154.6 ($C^{imid\text{-}2}$), 142.5 ($C^{B10a/B10b}$), 142.0 ($C^{B10a/B10b}$), 137.1 ($C^{B4a/B6a}$), 133.1 (C^{A3}), 132.8 (C^{A2}), 132.1 (C^{B7}), 131.4 (C^{B4}), 130.6 (C^{A1}), 126.9 (C^{B8}), 126.4 (C^{B3}), 125.0 (C^{A4}), 124.8 ($C^{B4a/B6a}$), 123.9 (C^{B6}), 120.0 (C^{B5}), 47.5 (C^{NCH_2}), 32.2 (C^{CH_2}), 29.4 ($2C^{CH_2}$), 26.6 (C^{CH_2}), 25.8 ($2C^{Me\text{-}phen}$), 23.3 (C^{CH_2}), 14.3 ($C^{Me\text{-}octyl}$). UV-Vis (CH_2Cl_2, 1.00×10^{-5} mol dm^{-3}) λ / nm (ε / dm^3 mol^{-1} cm^{-1}) 282 (87200), 304 (95300), 474 (13400). ESI MS *m/z*: 1093.7 $[M\text{-}PF_6]^+$ (calc. 1093.3). Found C 57.02, H 5.38, N 9.01; $C_{58}H_{62}Br_2CuF_6N_8P$ requires C 56.20, H 5.04, N 9.04%.

[Cu(3)$_2$][PF$_6$]. The method and purification were as for $[Cu(\mathbf{1})_2][PF_6]$; reagents and solvents were $[Cu(MeCN)_4][PF_6]$ (12.5 mg, 0.0334 mmol) in MeCN (2 ml) and **3** (50 mg, 0.0668 mmol) in $CHCl_3$ (2 ml). $[Cu(\mathbf{3})_2][PF_6]$ was isolated as a red solid (41.4 mg, 24.3 μmol, 72.7%). ^{1}H NMR (500 MHz, $CDCl_3$) δ / ppm 9.24 (br, 2H, H^{B7}), 8.85 (d, J = 8.6 Hz, 2H, H^{B4}), 7.94 (d, J = 8.5 Hz, 2H, H^{B3}), 7.78 (d, J = 8.3 Hz, 2H, H^{B8}), 7.54 (m, 4H, H^{A2}), 7.15 (m, 8H, H^{C2}), 7.07 (m, 4H, H^{A3}), 6.89 (m, 8H, H^{C3}), 4.78 (t, J = 6.8 Hz, 4H, H^{NCH_2}), 3.97 (t, J = 6.4 Hz, 8H, H^{OCH_2}), 2.45 (s, 6H, $H^{Me\text{-}phen}$), 2.43 (s, 6H, $H^{Me\text{-}phen}$), 2.00 (m, 4H, $H^{NCH_2C\boldsymbol{H}_2}$), 1.79 (m, 8H, $H^{OCH_2C\boldsymbol{H}_2}$), 1.52 (m, 8H, $H^{OCH_2CH_2C\boldsymbol{H}_2}$), 1.31 (m, 4H, $H^{NCH_2CH_2C\boldsymbol{H}_2}$), 1.27–1.14 (m, 16H, $H^{CH_2\text{-}octyl}$), 0.99 (t, J = 7.4 Hz, 12H, $H^{Me\text{-}butyl}$), 0.84 (t, J = 6.8 Hz, 6H, $H^{Me\text{-}octyl}$). ^{13}C NMR (126 MHz, $CDCl_3$) δ / ppm 156.1 (C^{C4}), 155.3 ($C^{B2/B9}$), 155.2 ($C^{imid\text{-}2}$), 154.8 ($C^{B2/B9}$), 150.4 (C^{A4}), 141.1 (C^{B10b}), 139.6 (C^{C1}), 131.7 (C^{B7}), 130.5 (C^{A2}), 129.9 (C^{B4}), 127.4 (C^{C2}), 125.6 (C^{B3}), 125.3 (C^{B8}), 124.8 (C^{B5}), 122.8 (C^{B6a}), 120.0 (C^{A1}), 119.2 (C^{B4a}), 118.8 (C^{A3}), 115.6 (C^{C3}), 67.8 (C^{OCH_2}), 46.7 (C^{NCH_2}), 31.6 ($C^{CH_2\text{-}octyl}$), 31.2 ($C^{OCH_2CH_2}$), 30.0 ($C^{NCH_2\boldsymbol{C}H_2}$), 29.0 ($C^{CH_2\text{-}octyl}$), 28.9 ($C^{CH_2\text{-}octyl}$), 26.0 ($C^{CH_2\text{-}octyl}$), 25.9 ($C^{Me\text{-}phen}$), 25.7 ($C^{Me\text{-}phen}$), 22.4 ($C^{CH_2\text{-}octyl}$), 18.9 ($C^{OCH_2CH_2\boldsymbol{C}H_2}$)), 13.9 ($C^{Me\text{-}octyl}$), 13.7 ($C^{Me\text{-}butyl}$), ($C^{B6}$, C^{B10a} not resolved). UV-Vis (CH_2Cl_2, 1.00×10^{-5} mol dm^{-3}) λ / nm (ε / dm^3 mol^{-1} cm^{-1}) 256 (73200), 292 (88800), 342 sh (58700), 469 (16100). HR ESI-MS *m/z*: 1557.8334 $[M–PF_6]^+$ (calc. 1557.8315). Satisfactory elemental analysis could not be obtained.

[Cu(4)$_2$][PF$_6$]. The method and purification were as for $[Cu(\mathbf{1})_2][PF_6]$; reagents and solvents were $[Cu(NCMe)_4][PF_6]$ (12.4 mg, 0.0332 mmol) in MeCN (5 mL) and **4** (40.0 mg, 0.0665 mmol) in CH_2Cl_2 (5 ml). $[Cu(\mathbf{4})_2][PF_6]$ was isolated as a dark red solid (46.9 mg, 0.0330 mmol, 100%). ^{1}H NMR (500 MHz, CD_3CN) δ / ppm: 9.18 (d, J = 8.2 Hz, 2H, H^{B7}), 8.99 (d, J = 8.6 Hz, 2H, H^{B4}), 8.27 (dt, J = 7.8, 1.0 Hz, 4H, H^{C4}), 8.11 (m, 4H, $H^{A2/A3}$), 7.97 (d, J = 8.5 Hz, 2H, H^{B3}), 7.94 (overlapping m, 6H, $H^{A2/A3+B8}$), 7.64 (m, 4H, H^{C1}), 7.51 (ddd, J = 8.3, 7.0, 1.2 Hz, 4H, H^{C2}), 7.36 (ddd, J = 8.0, 7.0, 0.9 Hz, 4H, H^{C3}), 4.90 (t, J = 7.2 Hz, 4H, H^{NCH_2}), 2.505 (s, 6H, $H^{Me\text{-}Phen}$), 2.50 (s, 6H, $H^{Me\text{-}Phen}$), 2.04 (m, 4H, $H^{NCH_2C\boldsymbol{H}_2}$), 1.30 (m, 4H, $H^{NCH_2CH_2C\boldsymbol{H}_2}$), 1.25–1.16 (m, 16H, $H^{CH_2\text{-}octyl}$), 0.76 (t, J = 6.9 Hz, 6H, $H^{Me\text{-}octyl}$). ^{13}C NMR (126 MHz, CD_3CN) δ / ppm 156.5 ($C^{B2/B9}$), 155.5 ($C^{B2/B9}$), 154.2 ($C^{imid\text{-}2}$), 141.5 (C^{B10b}), 141.1 (C^{B10a}), 140.6 (C^{C9a}), 139.0 (C^{A4}), 136.2 (C^{B6}), 131.7 (C^{A2}), 131.2 (C^{B7}), 130.6 (C^{B4}), 129.5 (C^{A1}), 127.3 (C^{A3}), 126.3 (C^{C2}), 126.0 (C^{B8}), 125.6 (C^{B3}), 125.3 (C^{B5}), 123.5 (C^{C4a}), 123.1 (C^{B6a}), 120.5 (C^{C4}), 120.3 (C^{C3}), 119.2 (C^{B4a}), 109.8 (C^{C1}), 46.6 (C^{NCH_2}), 31.3 ($C^{CH_2\text{-}octyl}$), 29.6 ($C^{NCH_2\boldsymbol{C}H_2}$), 28.5 ($2C^{CH_2\text{-}octyl}$), 25.6 ($C^{NCH_2CH_2\boldsymbol{C}H_2}$), 25.0 (overlapping $C^{Me\text{-}Phen}$), 22.3 ($C^{CH_2\text{-}octyl}$), 13.3 ($C^{Me\text{-}octyl}$). UV-Vis (CH_2Cl_2, 1.00×10^{-5} mol dm^{-3}) λ / nm (ε / dm^3 mol^{-1} cm^{-1}) 262 (106400), 292 (104300), 338 (52900), 475 (14500). ESI MS *m/z*: 1266.0 $[M–PF_6]^+$ (calc. 1265.6). HR ESI-MS: *m/z* 1265.5687 $[M–PF_6]^+$ (calc. 1265.5701). Found C 69.00, H 5.78, N 9.74; $C_{82}H_{78}CuF_6N_{10}P \cdot 0.5H_2O$ requires C 69.30, H 5.60, N 9.86%.

[Cu(5)$_2$][PF$_6$]. A solution of [Cu(NCMe)$_4$][PF$_6$] (22.8 mg, 0.0612 mmol) in MeCN (2 mL) was added dropwise to a solution of **28** (85.0 mg, 0.122 mmol) in $CHCl_3$ (2 mL). The dark red solution was stirred for 0.5 h and the solvent was then removed. The residue was suspended in water and the mixture then filtered. The filter cake was collected by dissolving it in a mixture of MeCN and $CHCl_3$ and then filtering the solution through a P3 glass filter (16-40 μm). After removing the solvent from the filtrate *in vacuo*, [Cu(**5**)$_2$][PF$_6$] was isolated as a red solid (91.0 mg, 0.057 mmol, 93.0%). ^{1}H NMR (500 MHz, CD_2Cl_2) δ / ppm 8.21 (br, 4H, H^{B5}), 7.72 (br, 4H, H^{B3}), 7.51 (m, 8H, H^{C2}), 7.35 (m, 16H, H^{A3}), 7.23 (m, 24H, H^{A2+C3}), 7.14 (m, 8H, H^{A4}), 2.53 (s, 12H, H$^{Me\text{-}phen}$). ^{13}C NMR (126 MHz, CD_2Cl_2) δ / ppm 157.2 (C^{B2}), 149.6 (C^{B4}), 149.3 (C^{C4}), 147.5 (C^{A1}), 144.5 (C^{B10a}), 131.0 (C^{C2}), 130.0 (C^{A3}), 126.0 (C^{B4a}), 125.8 (C$^{C3/A2}$), 125.7 (C^{B3}), 124.4 (C^{A4}), 122.5 (C$^{C3/A2}$), 124.1 (C^{B5}), 26.2 (C$^{Me\text{-}phen}$), (C^{C1} not resolved). UV-Vis (CH_2Cl_2, 1.00×10^{-5} mol dm^{-3}) λ / nm (ε / dm^3 mol^{-1} cm^{-1}) 295 (119200), 384 (54000), 486 (23600). ESI MS *m/z*: 1452.1 [M-PF$_6$]$^+$ (calc. 1452.6). Found C 72.47, H 4.79, N 7.01; $C_{100}H_{76}CuF_6N_8P.3H_2O$ requires C 72.69, H 5.00, N 6.78%.

Crystallography.

Single crystal data were collected on a Bruker APEX-II diffractometer with data reduction, solution and refinement using the programs APEX[34] and CRYSTALS.[35] Structure analysis used Mercury v. 3.5.1.[36,37]

Compound 4. $C_{41}H_{39}N_5$, M = 601.79, colourless needle, triclinic, space group P–1, a = 11.7635(14), b = 11.8126(14), c = 12.2155(14) Å, α = 72.343(4), β = 86.285(4), γ = 83.168(4)°, U = 1605.25(18) Å^3, Z = 2, D_c = 1.245 Mg m^{-3}, μ(Cu-Kα) = 0.570 mm^{-1}, T = 123 K. Total 18881 reflections, 5769 unique, R_{int} = 0.027. Refinement of 5522 reflections (415 parameters) with $I > 2\sigma(I)$ converged at final $R1$ = 0.0375 ($R1$ all data = 0.0391), $wR2$ = 0.0416 ($wR2$ all data = 0.0477), gof = 1.1112. CCDC 1405837.

DSC fabrication and measurements

Solaronix Test Cell Titania Electrodes were used for the photoanodes. They were washed with miliQ H_2O and heated at 450° C for 30 min, then cooled to ≈80 °C and soaked in a 1.0 mM DMSO solution of **6** for 24 h at room temperature. After removal of the electrodes from the solution, they were washed with DMSO and EtOH and dried in a stream of N_2. Each functionalized electrode was then soaked for 3 days in a 0.1 mM MeCN solution of [Cu(L$_{ancillary}$)$_2$][PF$_6$] (L$_{ancillary}$ = **1–5**) at room temperature. The electrodes were removed from the dye-bath, washed with MeCN and dried in a stream of N_2.

N719 reference electrodes were made by dipping Solaronix Test Cell Titania Electrodes in a 0.3 mM EtOH solution of N719 (Solaronix) for 3 days. The electrodes were removed from the dye-bath, and were washed with EtOH and dried in a stream of N_2.

For the counter electrodes, Solaronix Test Cell Platinum Electrodes were used, and volatile organic impurities were removed by heating on a heating plate at 450 °C for 30 min.

The dye-covered TiO_2 electrode and Pt counter-electrode were combined using thermoplast hot-melt sealing foil (Solaronix Test Cell Gaskets, 60 μm) by heating while pressing them together. The electrolyte (LiI (0.1 M), I_2 (0.05 M), 1-methylbenzimidazole (0.5 M), 1-butyl-3-methylimidazolinium iodide (0.6 M) in 3-methoxypropionitrile) was introduced into the DSC by vacuum backfilling. The hole in the counter electrode was sealed with hot-melt sealing foil (Solaronix Test Cell Sealings) and a cover glass (Solaronix Test Cell Caps).

For each dye, duplicate DSCs were made and the cells were completely masked.[38,39] Measurements were made by irradiating the DSC from behind using a SolarSim 150 (Solaronix) light source previously calibrated with a silicon reference cell to 100 mW cm^{-2} (1 sun).

External quantum efficiency (EQE) measurements were made using a Spe-Quest quantum efficiency instrument from Rera Systems (Netherlands) with a 100 W halogen lamp (QTH) and a lambda 300 grating monochromator (Lot Oriel). The monochromatic light was modulated to 3Hz using a chopper wheel (ThorLabs). The cell response was amplified with a large dynamic range IV converter (CVI Melles Griot) and measured with a SR830 DSP Lock-In amplifier (Stanford Research).

Results and discussion

Synthesis and characterization of ancillary ligands 1–5

We have previously reported the preparation and characterization of the bromo-derivative **1** and subsequent Hartwig-Buchwald amination with diphenylamine to give **2** (Scheme 2).[26] The same strategy was used for the synthesis of **3**. 4,4'-Di-n-butoxydiphenylamine was prepared by a copper(I) iodide/L-proline catalysed[32] Ullmann coupling (Scheme 3a) and was then used in the Hartwig-Buchwald amination shown in Scheme 3b. Compound **3** was isolated in 51.2% yield. Attempts to prepare **4** by reaction of **1** with 9*H*-carbazole using Hartwig-Buchwald conditions led to very low yields of **4**; changing the catalyst from [Pd(dba)$_2$]/P^{t}Bu$_3$ to [Pd(OAc)$_2$]/P^{t}Bu$_3$ or [Pd(PPh$_3$)$_4$] gave mixtures from which pure **4** could not be separated. We therefore opted for the alternative route to **4** shown in Scheme 4. Compound **4a** was formed by treatment of 4-(9*H*-carbazol-9-yl)benzaldehyde with 2,9-dimethyl-1,10-phenanthroline-5,6-dione and NH_4OAc; subsequent alkylation of the imidazole gave **4** in 18.3% yield. The electrospray mass spectra of **3** and **4** exhibited ions arising from [M+H]$^+$, and the compounds were characterized by ^{13}C and ^{1}H NMR spectroscopies using COSY, NOESY, HMQC and HMBC techniques. The alkyl chain desymmetrizes the phen unit, giving rise to pairs of signals in both the ^{1}H and ^{13}C NMR spectra for H/C$^{B3/B8}$, H/C$^{B4/B7}$, and H/C$^{Me\text{-}phen}$. For example, the methyl groups in the ^{1}H NMR spectrum appear at δ 3.01 and 3.07 ppm in **3**, and δ 2.83 and 2.84 ppm in **4**. In contrast to **4**, the ^{1}H NMR spectrum of precursor **4a** (see experimental section) reflects the C_2 symmetry that results from the tautomerism of the imidazole ring.

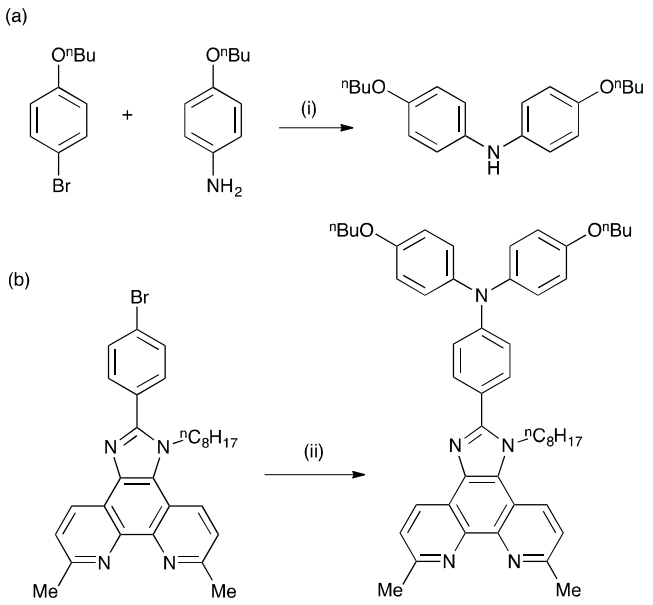

Scheme 3. (a) Synthetic route to 4,4'-di-*n*-butoxydiphenylamine; conditions (i) K_2CO_3, CuI, L-proline in DMSO, 90 °C, 24 h. (b) Conditions for Hartwig-Buchwald coupling to **3**: (ii) 4,4'-di-*n*-butoxydiphenylamine, NaO^tBu, catalytic $[Pd(dba)_2]/P^tBu_3$, toluene, reflux 15 h.

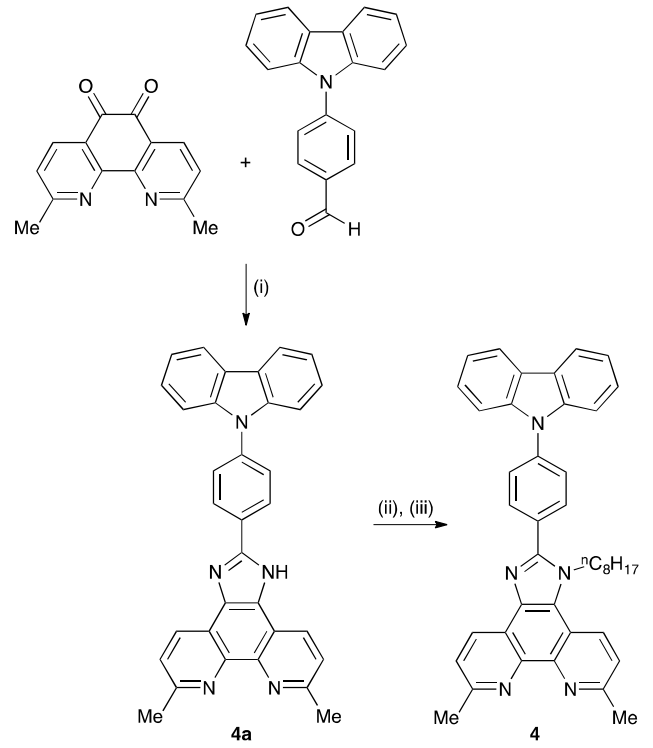

Scheme 4. Synthetic route to compound **4**; conditions (i) excess NH_4OAc, EtOH; (ii) NaH, DMF under N_2; (iii) $^nC_8H_{17}Br$, DMF, 75 °C, 15 h.

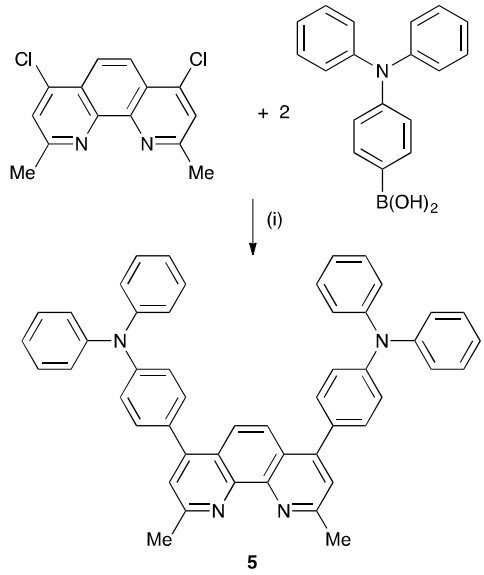

Scheme 5. Synthetic route to compound **5**; conditions (i) K_3PO_4, catalytic $[Pd(dba)_2]/P(C_6H_{11})_3$, 1,4-dioxane/$H_2O$ (ratio 5 : 2), reflux, 95 °C, 15 h.

The synthetic approach to compound **5** (Scheme 2) was based on that described in the patent literature for 4,7-bis(4-(diphenylamino)phenyl)-1,10-phenanthroline.[40] Suzuki coupling of 4,7-dichloro-2,9-dimethyl-1,10-phenanthroline with two equivalents of 4-(*N,N*-diphenylamino)phenylboronic acid (Scheme 5) gave **5** in moderate yield. The high-resolution electrospray mass spectrum confirmed the presence of the $[M+H]^+$ ion at *m/z* = 695.3174 $[M+H]^+$. Fig. 1 shows the ^1H NMR spectrum of **5** which is consistent with a C_2-symmetric molecule. Protons H^{B3} and H^{B5} were distinguished using the NOESY cross peak between H^{Me} and H^{B3}; H^{C2}/H^{B3} and H^{C2}/H^{B5} NOESY cross peaks were used to discriminate between H^{C2} and H^{C3}. Assignment of the ^{13}C NMR spectrum was made using HMBC and HMQC methods.

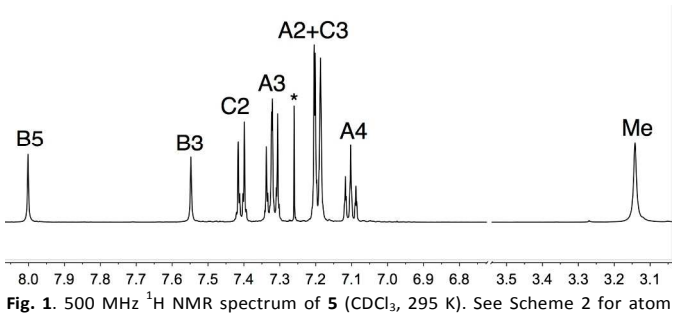

Fig. 1. 500 MHz ^1H NMR spectrum of **5** ($CDCl_3$, 295 K). See Scheme 2 for atom labelling; * is residual $CHCl_3$. Chemical shifts are in δ/ ppm.

The solution absorption spectra of the five ligands are compared in Fig. 2. Introduction of the diphenylamino or carbazole units on going from **1** to **2**, **3** or **4** enhances the photoresponse of the ligands in the region between 325 and 400 nm, but the most significant improvement in absorption towards the red-region is observed in compound **5** which absorbs down to ≈550 nm.

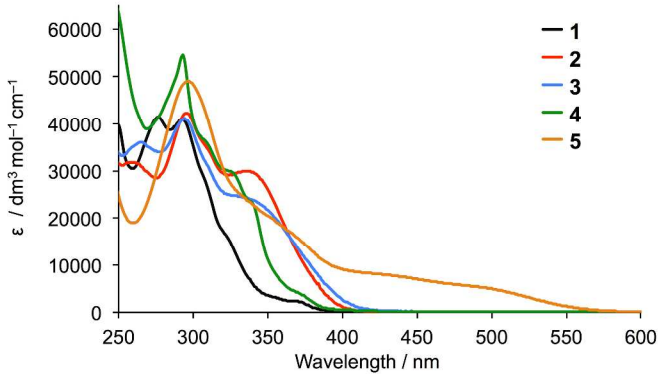

Fig. 2. Solution absorption spectra of ligands **1–5** (CH_2Cl_2, 1×10^{-5} mol dm^{-3}).

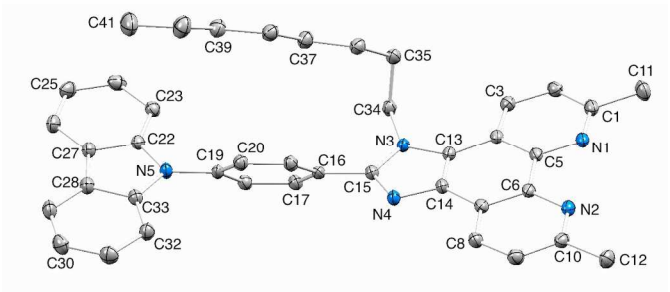

Fig. 3. Crystal structure of **4** with H atoms omitted and ellipsoids plotted at 50% probability level. Selected bond lengths: N1–C1 = 1.3250(14), N1–C5 = 1.3529(13), N2–C6 = 1.3551(14), N2–C10 = 1.3271(14), N3–C13 = 1.3892(13), N3–C15 = 1.3783(13), N3–C34 = 1.4644(13), N4–C14 = 1.3758(13), N4–C15 = 1.3152(14), N5–C19 =1.4216(13), N5–C22 = 1.3905(13), N5–C33 = 1.3954(13) Å.

Single crystal structure of 4

The single crystal structure of **4** was determined from crystals grown from a DMSO-d_6 solution in an NMR tube. The compound crystallizes in the triclinic space group *P*–1 and the structure is shown in Fig. 3. Bond lengths (caption to Fig. 3) and bond angles are unremarkable, and the phenyl ring containing C19 is twisted through 53.4° with respect to the plane through the imidazole ring consistent with minimizing inter-ring H...H contacts. The *n*-octyl chain is folded over the *N*-phenylcarbazole unit (Fig. 3), with an orientation which mimics that in **1**[26] and this leads to close CH_{alkyl}...π contacts, both to the phenyl spacer (CH...centroid = 3.47 Å) and to the heterocyclic ring of the carbazole (CH...centroid = 3.32 Å). Two packing motifs are of importance. Firstly, carbazole and phen units in adjacent molecules engage in face-to-face π-stacking interactions, leading to the assembly of chains parallel to the *c*-axis (Fig. 4a). As Fig. 3a illustrates, the carbazole and phen units are slipped with respect to one another giving an optimum configuration for π-interactions; the $carbazole_{centroid}$...$phen_{plane}$ distance is 3.40 Å. Adjacent chains interact through π-stacking and this is best described in terms of the quadruple-decker stack shown in Fig. 3b. The central interaction is between a centrosymmetric pair of 1*H*-phenanthro[9,10-*d*]imidazole domains (interplane separation = 3.33 Å). Extension beyond the quadruple-decker unit is prevented by the CH...π contacts from the terminal methyl group of the *n*-octyl chain (Fig. 4b).

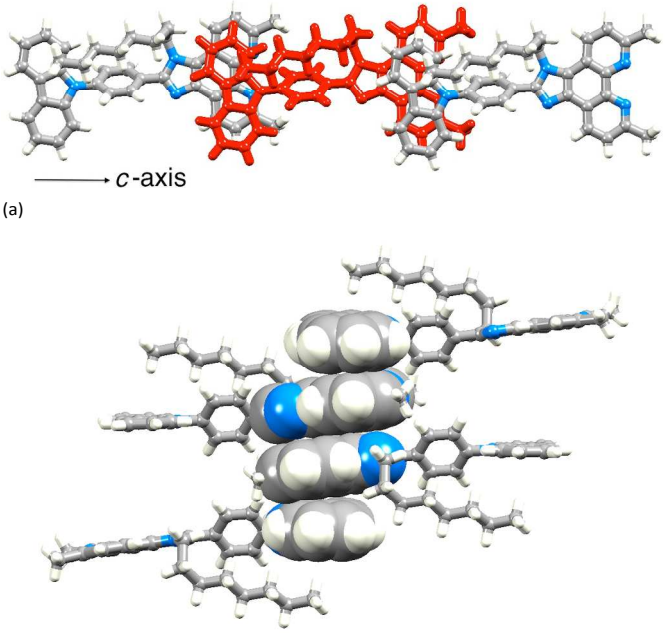

Fig. 4. (a) In **4**, chains run along the *c*-axis, assembled through π-stacking interactions between phen and carbazole units. (b) One quadruple-decker π-stack in **4**.

Synthesis and characterization of homoleptic copper complexes

The copper(I) complexes $[CuL_2][PF_6]$ with L = **1, 3–5** were prepared by dropwise addition of an MeCN solution of $[Cu(MeCN)_4][PF_6]$ to a solution of the ligand in $CHCl_3$ or CH_2Cl_2. The preparation of $[Cu(\mathbf{2})_2][PF_6]$ has previously been reported.[26] The homoleptic complexes were isolated in 70.5–100% yield, and in the electrospray mass spectrum of each, the highest mass peak envelope corresponded to the $[M–PF_6]^+$ ion. ^1H and ^{13}C NMR spectra were assigned using COSY, NOESY, HMQC and HMBC methods (Fig. S1†). Differing solubility properties of free ligands and complexes precluded the use of common solvents for recording NMR spectra of ligands and copper(I) complexes. Nonetheless, the shifts to higher frequencies for the signals of the phen unit (H^{B3}, H^{B8}, H^{B4} and H^{B7}) upon complexation are characteristic, as illustrated for **4** to $[Cu(\mathbf{4})_2][PF_6]$ in Fig. 5.

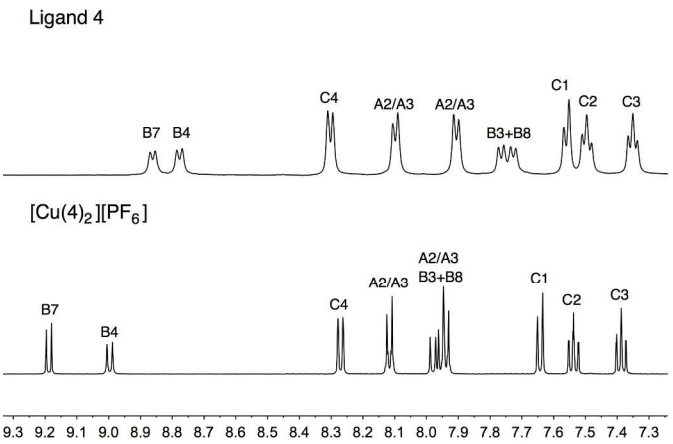

Fig. 5. Comparison of the aromatic regions of the 500 MHz ^{1}H NMR spectra of **4** (in DMSO-d_6) and [Cu(**4**)$_2$][PF$_6$] (in CD_3CN). See Scheme 2 for atom labelling.

The solution absorption spectra of [CuL$_2$][PF$_6$] with L = **1**–**5** are shown in Fig. 6. The approximate doubling in the values of the extinction coefficients for the high-energy, ligand-centred absorptions (assigned to $\pi^*\leftarrow\pi$ transitions) on going from L (Fig. 4) to $[CuL_2]^+$ (Fig. 6) is consistent with the formation of the homoleptic complexes. The absorption around 470–475 nm for [Cu(**1**)$_2$][PF$_6$], [Cu(**2**)$_2$][PF$_6$], [Cu(**3**)$_2$][PF$_6$] and [Cu(**4**)$_2$][PF$_6$] arises from metal-to-ligand charge transfer (MLCT) and this undergoes a bathochromic shift to 486 nm on going to [Cu(**5**)$_2$][PF$_6$]. The enhanced spectral response of [Cu(**5**)$_2$][PF$_6$] at wavelengths above 375 nm is noteworthy in terms of the incorporation of the {Cu(**5**)} unit in TiO_2-bound sensitizers (see later).

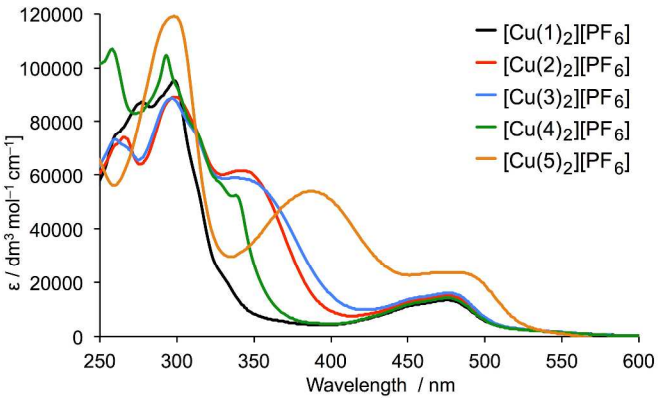

Fig. 6. Solution absorption spectra of complexes [CuL$_2$][PF$_6$] for L = **1–5** (CH_2Cl_2, 1 × 10^{-5} mol dm^{-3}).

The copper(I) complexes are redox active and cyclic voltammograms were recorded in CH_2Cl_2 to avoid possible involvement by coordinating solvents such as MeCN. [Cu(**1**)$_2$][PF$_6$] exhibits a reversible oxidation process (Fig. 7) at +0.48 V assigned to the Cu^+/Cu^{2+} redox couple. The value is close to the reported value of +0.50 V for 2,9-dimethyl-1,10-phenanthroline,[41] indicating that the 2-(4-bromophenyl)-1-octyl-1*H*-imidazo unit in **1** has little effect on the oxidation potential of the copper(I) centre. For [Cu(**2**)$_2$][PF$_6$], [Cu(**3**)$_2$][PF$_6$], [Cu(**4**)$_2$][PF$_6$] and [Cu(**5**)$_2$][PF$_6$], a number of quasi-reversible or irreversible oxidation processes were observed (Fig. S2†) consistent with the introduction of the diphenylamino or carbazole functionalizations; these were not investigated in detail. Ligand-based reduction processes are poorly defined (Fig. 7) for all the complexes.

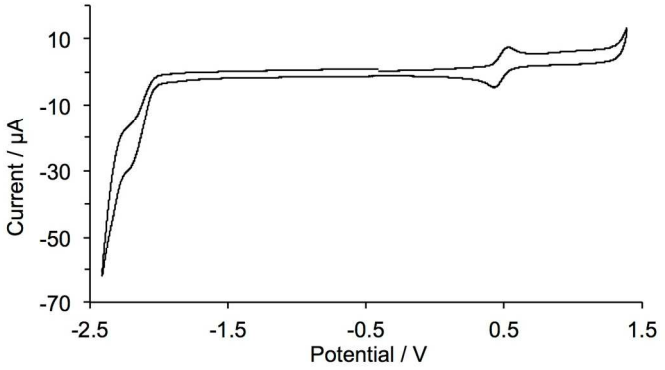

Fig. 7. Cyclic voltammogram of [Cu(**1**)$_2$][PF$_6$] in CH_2Cl_2 solution (E_{pc}–E_{pa} = 74 mV) with respect to Fc/Fc^+; scan rate = 0.1 V s^{-1}.

Preparation of DSCs and solid-state absorption spectra of dye-functionalized electrodes

The [Cu(L$_{anchor}$)(L$_{ancillary}$)]$^+$ dyes, in which L$_{anchor}$ is the phosphonic acid anchoring ligand **6**[42] (Scheme 6) and L$_{ancillary}$ is **1**–**5**, were assembled on TiO_2 electrodes by first soaking them in a solution of L$_{anchor}$ followed by immersion in solutions of [Cu(**1**)$_2$][PF$_6$], [Cu(**2**)$_2$][PF$_6$], [Cu(**3**)$_2$][PF$_6$], [Cu(**4**)$_2$][PF$_6$] or [Cu(**5**)$_2$][PF$_6$]. Dye-bath concentrations and dipping times were the same for all electrodes. Commercial TiO_2 electrodes with or without a scattering layer were used for DSC measurements or solid-state absorption spectroscopy, respectively. Electrodes with the reference dye N719 were prepared by soaking the TiO_2 electrodes in solutions of the sensitizer. Although we have previously shown that DSCs incorporating [Cu(**6**)(**2**)]$^+$ perform similarly using either I^-/I_3^- or $[Co(bpy)_3]^{2+/3+}$ electrolytes,[26] we chose in the present work to use a standard I^-/I_3^- electrolyte (see experimental section).

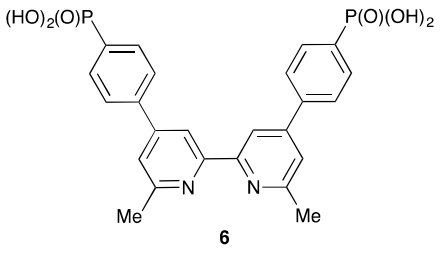

Scheme 6. Structure of the anchoring ligand **6**.

The solid-state absorption spectra of the sensitized electrodes are shown in Fig. 8; Fig. S3† shows photographs of the electrodes, all of which had the same soaking conditions in the dye baths. The values of λ_{max} for the MLCT bands of [Cu(**1**)$_2$]$^+$, [Cu(**2**)$_2$]$^+$, [Cu(**3**)$_2$]$^+$ and [Cu(**4**)$_2$]$^+$ in solution (470–

475 nm) are consistent with those of the on-surface dyes $[Cu(\mathbf{6})(\mathbf{1})]^+$, $[Cu(\mathbf{6})(\mathbf{2})]^+$, $[Cu(\mathbf{6})(\mathbf{3})]^+$ and $[Cu(\mathbf{6})(\mathbf{4})]^+$ (466–469 nm). Pleasingly, the enhanced absorption between 375–600 nm shown by $[Cu(\mathbf{5})_2]^+$ compared to the other homoleptic dyes in solution (Fig. 6) is also observed for the surface-anchored $[Cu(\mathbf{6})(\mathbf{5})]^+$ (Fig. 8). However, none of the dyes absorbs as far into the red as N719.

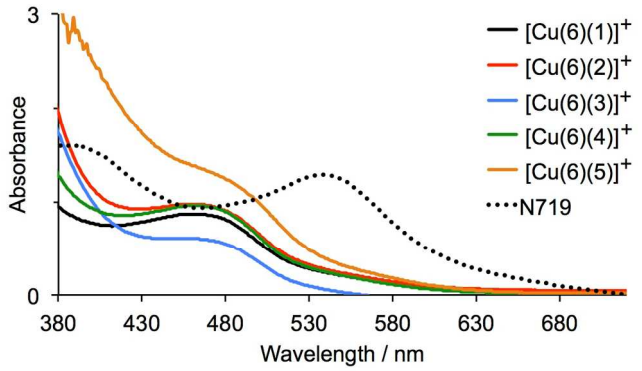

Fig. 8. Solid-state absorption spectra of dye-functionalized TiO_2 electrodes.

DSC performances

Table 1 gives the performance parameters for duplicate DSCs containing $[Cu(\mathbf{6})(\mathbf{1})]^+$, $[Cu(\mathbf{6})(\mathbf{2})]^+$, $[Cu(\mathbf{6})(\mathbf{3})]^+$, $[Cu(\mathbf{6})(\mathbf{4})]^+$ and $[Cu(\mathbf{6})(\mathbf{5})]^+$ on the day of assembly (day 0) and after 3 days. All DSCs show similar fill factors (*ff*) values. Values of the open-circuit voltage (V_{OC}) for all the copper(I) dyes lie in the range 523–562 mV on day 0 and show a small gain over a 3 day aging period (Table 1). Improved performance over time is a known phenomenon for copper(I)-containing dyes combined with an I^-/I_3^- electrolyte;[24] it has also been reported for ruthenium(II) dyes and appears to arise from disaggregation and reorganization of the surface-bound dye molecules.[43] For DSCs with $[Cu(\mathbf{6})(\mathbf{1})]^+$, $[Cu(\mathbf{6})(\mathbf{2})]^+$, $[Cu(\mathbf{6})(\mathbf{3})]^+$, $[Cu(\mathbf{6})(\mathbf{4})]^+$ and $[Cu(\mathbf{6})(\mathbf{5})]^+$, the improved V_{OC} values are not complemented by an increase in the short-circuit current density (J_{SC}) over time, and the overall efficiencies (η) remain similar or decrease from day 0 to day 3 (Table 1).

An important point is that these studies can be used to validate comparisons between DSC data from our laboratory where we use both commercial electrodes and those made in-house. Images obtained using scanning electron microscopy confirm that the ≈9 μm thickness of the transparent layer of a commercial electrode[44] corresponds to 4-layers of in-house screen printed TiO_2. The values of J_{SC}, V_{OC}, *ff* and η of the DSCs with $[Cu(\mathbf{6})(\mathbf{2})]^+$ (Table 1) using commercial electrodes with scattering layer and an I^-/I_3^- electrolyte, compare favourably with parameters (J_{SC} = 5.11 mA cm^{-2}, V_{OC} = 574 mV, *ff* = 71%, η = 2.08%) for DSCs containing an I^-/I_3^- electrolyte with the dye $[Cu(\mathbf{6})(\mathbf{2})]^+$ anchored on 4-layer screen-printed electrodes post-treated with 40 mmol dm^{-3} H_2O-$TiCl_4$.[26]

The current density/potential (*J-V*) curves recorded on the day of device fabrication are shown in Fig. S4†; *J-V* curves for the best performing device from each pair of duplicate DSCs are displayed in Fig. 9. The DSCs sensitized with $[Cu(\mathbf{6})(\mathbf{5})]^+$ outperform the other solar cells, the main contributing factor being enhanced J_{SC} values. This is consistent with extended light absorption towards the red for complexes containing **5** (Fig. 8) and is confirmed by the higher external quantum efficiencies (EQE) of the DSCs. EQE spectra for all devices are shown Fig. S5†, and Fig. 10 depicts the spectra for the best performing DSC of each pair; values of EQE_{max} and λ_{max} are given in Table 2. Although the values of EQE_{max} for $[Cu(\mathbf{6})(\mathbf{1})]^+$ and $[Cu(\mathbf{6})(\mathbf{4})]^+$ are higher than for $[Cu(\mathbf{6})(\mathbf{5})]^+$ (Table 2), the extension of the EQE spectrum of the DSCs with $[Cu(\mathbf{6})(\mathbf{5})]^+$ to longer wavelengths (Fig. 10 and S5†) leads to higher J_{SC} values with respect to DSCs with the other dyes. Fig. S6† shows a comparison of the EQE spectra of duplicate DSCs containing $[Cu(\mathbf{6})(\mathbf{5})]^+$ with the EQE spectrum of an N719 sensitized DSC, and demonstrates the origins of the lower values of J_{SC} for the copper(I) dye versus the ruthenium(II) reference dye.

Table 1. Performance parameters of masked DSCs with the copper(I) dyes; two DSCs were fabricated for each dye. Data are compared to a DSC containing N719. See Schemes 2 and 6 for ligand structures.

Dye	On the day of sealing the DSCs				
	J_{SC} / mA cm^{-2}	V_{OC} / mV	*ff* / %	η / %	Relative η / %
$[Cu(\mathbf{6})(\mathbf{1})]^+$	5.38	542	71	2.08	25.8
$[Cu(\mathbf{6})(\mathbf{1})]^+$	5.82	547	72	2.30	28.6
$[Cu(\mathbf{6})(\mathbf{2})]^+$	5.41	562	75	2.29	28.4
$[Cu(\mathbf{6})(\mathbf{2})]^+$	4.71	558	73	1.92	23.9
$[Cu(\mathbf{6})(\mathbf{3})]^+$	4.75	523	73	1.81	22.5
$[Cu(\mathbf{6})(\mathbf{3})]^+$	5.65	540	68	2.07	25.7
$[Cu(\mathbf{6})(\mathbf{4})]^+$	5.82	556	73	2.35	29.1
$[Cu(\mathbf{6})(\mathbf{4})]^+$	5.89	562	72	2.38	29.5
$[Cu(\mathbf{6})(\mathbf{5})]^+$	6.81	557	72	2.73	33.9
$[Cu(\mathbf{6})(\mathbf{5})]^+$	6.40	558	73	2.62	32.5
N719	17.94	642	70	8.06	100.0
	3 days after sealing the DSCs				
	J_{SC} / mA cm^{-2}	V_{OC} / mV	*ff* / %	η / %	Relative η / %
$[Cu(\mathbf{6})(\mathbf{1})]^+$	5.32	548	71	2.06	24.3
$[Cu(\mathbf{6})(\mathbf{1})]^+$	5.57	555	72	2.23	26.3
$[Cu(\mathbf{6})(\mathbf{2})]^+$	4.84	570	75	2.06	24.3
$[Cu(\mathbf{6})(\mathbf{2})]^+$	4.24	567	72	1.74	20.4
$[Cu(\mathbf{6})(\mathbf{3})]^+$	4.47	539	72	1.73	20.4
$[Cu(\mathbf{6})(\mathbf{3})]^+$	5.11	546	68	1.88	22.2
$[Cu(\mathbf{6})(\mathbf{4})]^+$	5.54	558	72	2.22	26.1
$[Cu(\mathbf{6})(\mathbf{4})]^+$	5.26	570	71	2.14	25.2
$[Cu(\mathbf{6})(\mathbf{5})]^+$	6.47	567	71	2.59	30.5
$[Cu(\mathbf{6})(\mathbf{5})]^+$	6.17	564	73	2.54	30.0
N719	17.77	700	68	8.49	100.0

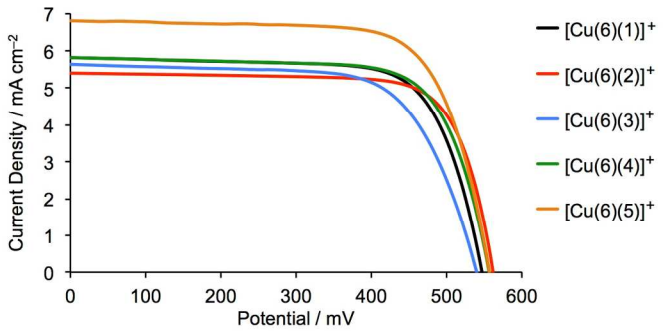

Fig. 9. *J-V* curves for DSCs containing the sensitizers [Cu(**6**)(**1**)]$^+$, [Cu(**6**)(**2**)]$^+$, [Cu(**6**)(**3**)]$^+$, [Cu(**6**)(**4**)]$^+$ and [Cu(**6**)(**5**)]$^+$; see also Fig. S4†. Data were recorded on the day of DSC fabrication.

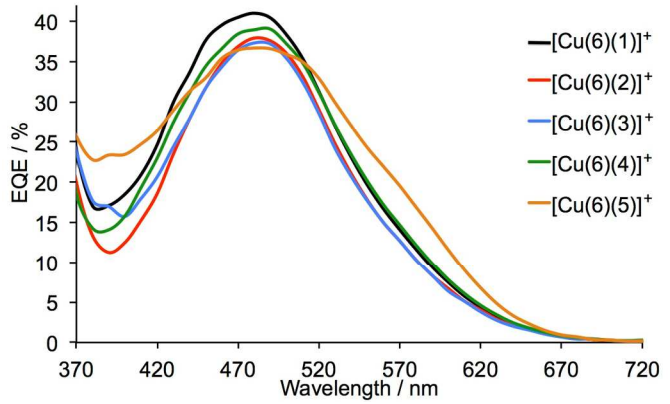

Fig. 10. EQE spectra of DSCs containing the sensitizers [Cu(**6**)(**1**)]$^+$, [Cu(**6**)(**2**)]$^+$, [Cu(**6**)(**3**)]$^+$, [Cu(**6**)(**4**)]$^+$ and [Cu(**6**)(**5**)]$^+$; see also Fig. S5†. The spectra were recorded 3 days after cell assembly.

Table 2. EQE maxima for two independent sets of DSCs containing dyes [Cu(**6**)(L$_{ancillary}$)]$^+$ with L$_{ancillary}$ = **1–5** measured 3 days after cell fabrication.

Anchored dye	EQE$_{max}$ / %	λ_{max} / nm
[Cu(**6**)(**1**)]$^+$	41.0	480
[Cu(**6**)(**1**)]$^+$	39.4	480
[Cu(**6**)(**2**)]$^+$	37.9	480
[Cu(**6**)(**2**)]$^+$	35.3	480
[Cu(**6**)(**3**)]$^+$	37.3	480
[Cu(**6**)(**3**)]$^+$	34.7	480
[Cu(**6**)(**4**)]$^+$	39.0	480
[Cu(**6**)(**4**)]$^+$	39.1	480
[Cu(**6**)(**5**)]$^+$	36.6 (sh. 19.5)	490 (sh. 570)
[Cu(**6**)(**5**)]$^+$	37.1 (sh. 19.5)	490 (sh. 570)
N719	74.4	530

Conclusions

We have reported the synthesis and characterization of a series of homoleptic [Cu(L)$_2$][PF$_6$] complexes in which L is a 2,9-dimethyl-1,10-phenanthroline substituted in either the 5,6-positions with a peripherally-functionalized imidazole unit or in the 4,7-positions with electron-donating 4-(diphenylamino)phenyl groups. The solution absorption spectrum of [Cu(**5**)$_2$][PF$_6$] exhibits a greater spectral response above 375 nm than those of [Cu(**1**)$_2$][PF$_6$], [Cu(**2**)$_2$][PF$_6$], [Cu(**3**)$_2$][PF$_6$] and [Cu(**4**)$_2$][PF$_6$]. The heteroleptic dyes [Cu(**6**)(L)]$^+$ were assembled in a stepwise manner on TiO$_2$ electrodes, and solid-state absorption spectra confirmed enhanced absorption between 375–600 nm for [Cu(**6**)(**5**)]$^+$ compared to [Cu(**6**)(**1**)]$^+$, [Cu(**6**)(**2**)]$^+$, [Cu(**6**)(**3**)]$^+$ and [Cu(**6**)(**4**)]$^+$. Comparison of the performances of DSCs containing [Cu(**6**)(**2**)]$^+$, [Cu(**6**)(**3**)]$^+$ and [Cu(**6**)(**4**)]$^+$ with those with [Cu(**6**)(**1**)]$^+$ suggests only a marginal influence of the diphenylamine or carbazole hole-transporting domains in 5,6-substituted phenanthroline dyes. In ancillary ligand **5**, the 4-(diphenylamino)phenyl hole-transporting units are introduced directly into the 4- and 7-positions of the phen unit, and this combined with a phosphonic anchoring domain in [Cu(**6**)(**5**)]$^+$ leads to the best performing DSCs of those investigated. Although the values of EQE$_{max}$ for [Cu(**6**)(**1**)]$^+$ and [Cu(**6**)(**4**)]$^+$ exceed that of [Cu(**6**)(**5**)]$^+$, the extension of the EQE spectrum of the DSCs with [Cu(**6**)(**5**)]$^+$ towards the red-end of the spectrum results in higher J_{SC} values with respect to DSCs with the other dyes. We are currently exploring the effects on DSC performance of introducing other substituents in the 4,7-positions of 2,9-dimethyl-1,10-phenanthrolines used as ancillary ligands in heteroleptic copper(I) sensitizers, and are also focusing on electrolyte optimization.

Acknowledgements

We acknowledge financial support from the European Research Council (Advanced Grant 267816 LiLo), the Swiss National Science Foundation (Grant 200020_144500) and the University of Basel.

Notes and references

Department of Chemistry, University of Basel, Spitalstrasse 51, CH-4056 Basel, Switzerland. E-mail: catherine.housecroft@unibas.ch; Tel: +41 61 267 1008.

† Electronic Supplementary Information (ESI) available: Fig. S1: Representative HMQC and HMBC spectra. Fig. S2: cyclic voltammograms of copper(I) complexes; Fig. S3: photographs of dye-functionalized electrodes; Figs. S4–S6: *J-V* curves and EQE spectra. See DOI: 10.1039/b000000x/

1 B. O'Regan and M. Grätzel, *Nature*, 1991, **353**, 737.

2 G. C. Vougioukalakis, A. I. Philippopoulos, T. Stergiopoulos and P. Falaras, *Coord. Chem. Rev*., 2011, **255**, 2602.
3 A. Mishra, M. K. R. Fischer and P. Bäuerle, *Angew. Chem. Int. Ed*., 2009, **48**, 2474.
4 L.-L. Li and E. W.-G. Diau, *Chem. Soc. Rev*., 2013, **42**, 291.
5 A. Yella, H.-W. Lee, H. N. Tsao, C. Yi, A. K. Chandiran, Md. K. Nazeeruddin, E. W.-G. Diau, C.-Y. Yeh, S. M Zakeeruddin and M. Grätzel, *Science*, 2011, **334**, 629; M. Zhang, Y. Wang, M. Xu, W. Ma, R. Li and P. Wang *Energy Environ. Sci.*, 2013, **6**, 2944; K. Kakiage, Y. Aoyama, T. Yano, T. Otsuka, T. Kyomen, M. Unno and M. Hanaya, *Chem. Commun*., 2014, **50**, 6379; H. Ozawa, Y. Okuyama and H. Arakawa, *ChemPhysChem*, 2014, 15, 1201.
6 Z. Lin, N.-G. Park and G. Li, *J. Mater. Chem. A*, 2015, **3**, 8924 and papers in this perovskite-themed issue of the journal.
7 N. J. Jeon, J. H. Noh, W. S. Yang, Y. C. Kim, S. Ryu, J. Seo and S. I. Seok, *Science*, 2015, **348**, 1234.
8 W. S. Yang, J. H. Noh, N. J. Jeon, Y. C. Kim, S. Ryu, J. Seo and S. I. Seok, *Nature*, 2015, **517**, 476.
9 B. Bozic-Weber, E. C. Constable and C. E. Housecroft, *Coord. Chem. Rev.*, 2013, **257**, 3089.
10 T. Bessho, E. C. Constable, M. Graetzel, A. Hernandez Redondo, C. E. Housecroft, W. Kylberg, Md. K. Nazeeruddin, M. Neuburger and S. Schaffner, *Chem. Commun,* 2008, 3717; B. Bozic-Weber, E. C. Constable, C.E. Housecroft, P. Kopecky, M. Neuburger and J. A. Zampese, *Dalton Trans.* 2011, **40**, 12584.
11 N. Alonso-Vante, J.-F. Nierengarten and J.-P. Sauvage, *J. Chem. Soc., Dalton Trans.*,1994, 1649.
12 F. J. Malzner, S. Y. Brauchli, E. C. Constable, C. E. Housecroft and M. Neuburger, *RSC Adv.*, 2014, **4**, 48712.
13 M. Sandroni, L. Favereau, A. Planchat, H. Akdas-Kilig, N. Szuwarski, Y. Pellegrin, E. Blart, H. Le Bozec, M. Boujtita and F. Odobel, *J. Mater. Chem. A*, 2014, **2**, 9944.
14 A. Colombo, C. Dragonetti, M. Magni, D. Roberto, F. Demartin, S. Caramori and C. A. Bignozzi, *ACS Appl. Mater. Interfaces*, 2014, **6**, 13945.
15 See for example: S. Sakaki, T. Kuroki and T. Hamada, *J. Chem. Soc., Dalton Trans.,* 2002, 840; E. C. Constable, A. Hernandez Redondo, C. E. Housecroft, M. Neuburger and S. Schaffner, *Dalton Trans.*, 2009, 6634; B. Bozic-Weber, E. C. Constable, C. E. Housecroft, M. Neuburger and J. R. Price, *Dalton Trans.*, 2010, **39**, 3585; A. Colombo, C. Dragonetti, D. Roberto, A. Valore, P. Biagini and F. Melchiorre, *Inorg. Chim. Acta*, 2013, **407**, 204
16 M. Mohamkumar, F. Monti, M. Holler, F. Niess, B. Delavaux-Nicot, N. Armaroli, J.-P. Sauvage and J.-F. Nierengarten. *Chem. Eur. J.*, 2014, **20**, 12083 and references therein.
17 See for example: M. Schmittel and A. Ganz, *Chem. Commun.*, 1997, 999; M. Schmittel, H. Ammon, V. Kalsani, A. Wiegrefe and C. Michel, *Chem. Commun*., 2002, 2566.
18 M. Sandroni, M. Kayanuma, A. Planchat, N. Szuwarski, E. Blart, Y. Pellegrin, C. Daniel, M. Boujtita and F. Odobel, *Dalton. Trans*., 2013, **42**, 10818.
19 A. Hernandez Rendondo, E. C. Constable and C. E. Housecroft, *Chimia*, 2009, **63**, 205.
20 E. Schönhofer, B. Bozic-Weber, C. J. Martin, E. C. Constable, C. E. Housecroft and J. A. Zampese, *Dyes and Pigments,* 2015, **115**, 154.
21 N. Hostettler, S. O. Fürer, B. Bozic-Weber, E. C. Constable and C. E. Housecroft, *Dyes and Pigments,* 2015, **116**, 124.
22 S. Y. Brauchli, F. J. Malzner, E. C. Constable and C. E. Housecroft, *RSC Adv*., 2015, **5**, 48516 and references therein.
23 N. Hostettler, I. A. Wright, B. Bozic-Weber, E. C. Constable and C. E. Housecroft, *RSC Adv*., 2015, **5**, 37906 and references therein.
24 S. Y. Brauchli, F. J. Malzner, E. C. Constable and C. E. Housecroft, *RSC Adv.*, 2014, **4**, 62728 and references therein.
25 See for example: Y.-C. Hsu, H. Zheng, J. T. Lin and K. C. Ho, *Solar Energy Mater. Solar Cells*, 2005, **87**, 357; J.-F. Yin, D. Bhattacharya, Y.-C. Hsu, C.-C. Tsai, K.-L. Lu, H. C. Lin, J.-G. Chen and K.-C. Ho, *J. Mater. Chem.*, 2009, **19**, 7036; S.-H. Fan, A.-G. Zhang, C.-C. Ju, L.-H. Gao and K.-Z. Wang, *Inorg. Chem.*, 2010, **49**, 3752; S.-H. Fan, A.-G. Zhang, C.-C. Ju, L.-H. Gao and K.-Z. Wang, *Solar Energy*, 2011, **85**, 2497; Q.-Y. Yu, J.-F. Huang, Y. Shen, L.-M. Xiao, J.-M. Liu, D.-B. Kuang and C.-Y. Su, *RSC Adv.*, 2013, **3**, 19311.
26 B. Bozic-Weber, E. C. Constable, S. O. Fürer, C. E. Housecroft, L. J. Troxler and J. A. Zampese, *Chem. Commun.*, 2013, **49**, 7222.
27 See for example: J. E. Kroeze, N. Hirata, S. Koops, Md. K. Nazeeruddin, L. Schmidt-Mende, M. Grätzel and J. R. Durrant, *J. Am. Chem. Soc.*, 2006, **128**, 16376; Y. Ooyama and Y. Harima, *Eur. J. Org. Chem.*, 2009, 2903; W. H. Nguyen, C. D. Bailie, J. Burschka, T. Moehl, M. Grätzel, M. D. McGehee and A. Sellinger, *Chem. Mater.*, 2013, **25**, 1519; Q. Feng, G. Zhou and Z.-S. Wang, *J. Power Sources*, 2013, **239**, 16; K. Omata, S. Kuwahara, K. Katayama, S. Qing, T. Toyoda, K.-M. Lee and C.-G. Wu, *Phys. Chem. Chem. Phys.*, 2015, **17**, 10170 and references therein.
28 R. H. Zheng, H. C. Guo, H. J. Jiang, K. H. Xu, B. B. Liu, W. L. Sun and Z. Q. Shen, *Chinese Chem. Lett.*, 2010, **21**, 1270.

29 K. Guzow, M. Czerwińska, A. Ceszlak, M. Kozarzewska, M. Szabelski, C. Czaplewski, A. Łukaszewicz, A. Kubicki and W. Wiczk, *Photochem. Photobiol. Sci.*, 2013, **12**, 284.
30 A. F. Larsen and T. Ulven, *Org. Lett.*, 2011, **13**, 3546.
31 G. J. Kubas, *Inorg. Synth*., 1990, **28**, 68.
32 M. Shallaiah, Y. C. Rajan and H.-C. Lin, *J. Mater. Chem*., 2012, **22**, 8976.
33 S. A. Odom, K. Lancaster, L. Beverina, K. M. Lefler, N. J. Thompson, V. Coropceanu, J.-L. Brédas, S. R. Marder and S. Barlow, Chem. Eur. J., 2007, **34**, 9637.
34 Bruker Analytical X-ray Systems, Inc., 2006, APEX2, version 2 User Manual, M86-E01078, Madison, WI.
35 P. W. Betteridge, J. R. Carruthers, R. I. Cooper, K. Prout and D. J. Watkin, *J. Appl. Cryst.*, 2003, **36**, 1487.
36 I. J. Bruno, J. C. Cole, P. R. Edgington, M. K. Kessler, C. F. Macrae, P. McCabe, J. Pearson and R. Taylor, *Acta Crystallogr., Sect. B* 2002, **58**, 389.
37 C. F. Macrae, I. J. Bruno, J. A. Chisholm, P. R. Edgington, P. McCabe, E. Pidcock, L. Rodriguez-Monge, R. Taylor, J. van de Streek and P. A. Wood, *J. Appl. Cryst.*, 2008, **41**, 466.
38 H. J. Snaith, *Energy Environ. Sci.*, 2012, **5**, 6513.
39 H. J. Snaith, *Nature Photonics*, 2012, **6**, 337.
40 N. Herron, M. A. Guidry, V. Rostovtsev, W. Gao, Y. Wang, Y. Shen and J. A. Merlo, Appl. number PCT/US2009/069184 (International Publication Number WO 2010/075379 A2).
41 M. K. Eggleston,D. R. McMillin, K. S. Koenig and A. J. Pallenberg, *Inorg. Chem.*, 1997, **36**, 172.
42 B. Bozic-Weber, S. Y. Brauchli, E. C. Constable, S. O. Fürer, C. E. Housecroft, F. J. Malzner, I. A. Wright and J. A. Zampese, *Dalton Trans*., 2013, **42**, 12293.
43 B. Wenger, M. Grätzel and J.-E. Moser, *J. Am. Chem. Soc.*, 2005, **127**, 12150; B. Wenger, M. Grätzel and J.-E. Moser, *Chimia*, 2005, **59**, 123; V. K. Thorsmølle, B. Wenger, J. Teuscher, C. Bauer and J.-E. Moser, *Chimia*, 2007, **61**, 631.
44 S. Y. Brauchli, B. Bozic-Weber, E. C. Constable, N. Hostettler, C. E. Housecroft and J. A. Zampese, *RSC Adv.*, 2014, **4**, 34801.

